

The H1 Forward Proton Spectrometer at HERA

P.van Esch

Inter-University Institute for High Energies ULB-VUB, Brussels, Belgium

M.Kapichine, A.Morozov, V.Spaskov

Joint Institute of Nuclear Research, Dubna, Russia

W.Bartel, B.List¹, H.Mahlke-Krüger, V.Schröder, T.Wilksen

DESY, Hamburg, Germany

F.W.Büsser, K.Geske, O.Karschnik, F.Niebergall, H.Riege, J.Schütt,

R.van Staa, C.Wittek

II. Institut für Experimentalphysik, Universität Hamburg, Hamburg, Germany

D.Dau

Institut für Reine und Angewandte Kernphysik, Universität Kiel, Kiel, Germany

D.Newton

School of Physics and Chemistry, University of Lancaster, Lancaster, UK

S.K.Kotelnikov, A.Lebedev, S.Rusakov

Lebedev Physical Institute, Moscow, Russia

A.Astvatsatourov, J.Bähr, U.Harder, K.Hiller², B.Hoffmann³, H.Lüdecke,

R.Nahnauer

DESY Zeuthen, Zeuthen, Germany

¹Presently research associate at CERN.

²Corresponding author, Tel.: +49 33762 77208, Fax: +49 33762 77330, e-mail: hillar@ifh.de

³Now Berlin Chemie AG, 12489 Berlin, Glienicke Weg 125.

Abstract

The forward proton spectrometer is part of the H1 detector at the HERA collider. Protons with energies above 500 GeV and polar angles below 1 mrad can be detected by this spectrometer. The main detector components are scintillating fiber detectors read out by position-sensitive photo-multipliers. These detectors are housed in so-called Roman Pots which allow them to be moved close to the circulating proton beam. Four Roman Pot stations are located at distances between 60 m and 90 m from the interaction point.

PACS: 29.30.Aj, 29.40.Gx

Keywords: HERA, H1 detector, Roman pots, Scintillating fibers, Diffractive protons

1 Introduction

The forward proton spectrometer (FPS) is part of the H1 detector at the HERA collider at DESY [1]. From 1995, the first year of FPS operation, until 1997 HERA collided 27.5 GeV positrons with 820 GeV protons. In 1998 positrons were replaced by electrons¹ and the proton energy was increased to 920 GeV.

The aim of the FPS is to extend the acceptance of the H1 detector in the very forward direction, which is the direction of the outgoing proton beam. The central tracking chambers cover the angular range down to polar angles of 5° . At smaller angles energy deposits are observed in detectors close to the outgoing proton beam direction. The liquid argon calorimeter, the plug calorimeter and the proton remnant tagger in combination with the forward muon system are sensitive to forward activities down to polar angles of about 1 mrad [2]. The FPS has been built to measure forward going protons which are scattered at polar angles below this range.

Forward going protons with energies close to the kinematic limit of the incident proton beam energy arise from diffractive processes, which in Regge theory are described by Pomeron exchange [3]. At lower proton energies processes with meson exchange become the dominant production mechanism [4]. The measurement of diffractive processes offers the possibility to investigate the structure of the exchanges [5,6].

The FPS measures the trajectory of protons emerging from electron-proton collisions at the interaction point. The HERA magnets in the forward beam line separate scattered protons from the circulating proton beam. After a distance of about 60 m the scattered protons deviate typically a few millimeters from the central proton orbit and can be measured by tracking detectors.

These detectors are multi-layer scintillating fiber detectors read out by position-sensitive photo-multipliers (PSPMs). Scintillator tiles cover the sensitive detector area and are used to form trigger signals. To provide the necessary aperture for the proton injection into HERA the detectors are mounted in movable plunger vessels, so-called Roman Pots, which are retracted during the beam filling and orbit tuning process [7]. When stable conditions are reached the detectors are moved close to the circulating beam.

Due to the optics and the construction of the beam line only one secondary particle with at least 500 GeV energy can reach the FPS stations. The track parameters of the measured trajectories are used to reconstruct the energy and the scattering angles at the interaction point based on the knowledge of bending strengths and positions of the HERA magnets.

Four FPS stations at distances between 64 m and 90 m from the interaction point measure the trajectory of scattered protons. In 1995 two vertical stations were built, which approach the beam from above. They detect protons in the kinematic range

¹Throughout this paper electron is a generic name for e^- and e^+ .

$0.5 < E'/E_p < 0.95$, where E' and E_p are the energies of the scattered and the incident protons, respectively. In 1997 two horizontal stations were added, which approach the beam from the outer side of the proton ring. Complementary to the vertical FPS stations, they are sensitive in the range $E'/E_p > 0.9$.

This paper is organized as follows: section 2 contains the details of the FPS hardware components. In section 3 the operation of the FPS and the experience after three years of data taking are discussed. The main detector characteristics as acceptance, efficiency and resolution are given in section 4. In this section also the method of energy reconstruction and calibration are described. An summary of the relevant FPS parameters and an outlook on physics results is given in section 5.

2 Detector Components

The positions of the four FPS stations along the forward beam line are shown in fig.1. The two vertical stations are placed at 81 m and 90 m behind the BU00 dipole magnet, which bends the proton beam 5.7 mrad upwards. In front of this magnet at 64 m the first horizontal station is placed while the second horizontal station is located behind the BU00 magnet at 80 m.

2.1 Mechanics

All FPS stations consist of two major mechanical components: the plunger vessel which is the movable housing of the detector elements, and the fiber detectors with their readout components.

The plunger vessel is a cylinder made of 3 mm stainless steel. The inner volume, where the fiber detectors are mounted, has a diameter of 140 mm. To reduce the amount of material in front of the detectors thin windows of 0.3 mm steel are welded to the main cylinder. The bottom sections at the positions of the detectors are closed by 0.5 mm steel plates.

The plunger vessel can be moved close to the proton beam orbit due to the flexible connection via steel bellows to a flange of the beam pipe. In the vertical stations the plunger vessel is driven by spindles which are connected by a belt to a stepping motor. Due to space limitations the horizontal stations have a hydraulic moving system. The maximum range for the detector movement is 50 mm in the vertical stations and 35 mm in the horizontal stations. All stations are equipped with external position measuring devices ² which give the actual detector positions with 10 μ m precision. These values are recorded every second by the slow control system.

²Messtaster Metro MT60, Dr.J.Heidenhain GmbH, D-8225 Traunreut.

A sketch of the detector insert of the horizontal stations is shown in fig.2a. The detector carrier is an aluminum tube with a carbon fiber end part to support the fiber detectors. The platform above the detector carrier houses the PSPMs and the front-end electronics. The trigger photo-multipliers (PMTs) are fixed on the detector carrier inside the plunger vessel. In the vertical stations the basic arrangement is the same, but the trigger PMTs are placed outside the plunger vessel on the same platform as the PSPMs.

For the reconstruction of the proton energy the positions of all FPS stations with respect to the HERA proton beam have to be known. For this purpose a measuring plate with four marks is inserted into the plunger vessel. These marks are geodetically surveyed with a precision of $100\text{ }\mu\text{m}$. The position of the fiber detectors with respect to the outer marks is measured on a scanner with a precision of $20\text{ }\mu\text{m}$.

The front-end electronics together with the PSPMs and trigger PMTs has a power consumption of about 150 W. To keep the temperature below 30°C the walls of the platform housing the electronic components are water cooled.

The front-end electronics of all FPS stations is surrounded by an external lead shielding against synchrotron radiation. The horizontal stations have in addition a soft iron shielding to reduce the influence of magnetic stray fields on the PSPMs.

For safety reasons the plunger vessels are filled with dry nitrogen gas, so that in case of leakage only a small amount of dry gas enters the HERA machine vacuum.

2.2 Fiber Detectors

Scintillating fibers arranged in multi-layer structures represent a fast and robust tracking detector. The vertex smearing and beam divergence at the interaction point set the scale for the spatial detector resolution. Due to these constraints, the energy resolution cannot be improved by a detector resolution better than $100\mu\text{m}$.

A view of the arrangement of the fiber detectors in the vertical stations is given in fig.2b. Each pot is equipped with two identical subdetectors measuring two coordinates transverse to the beam direction. The subdetectors are separated by 60 mm to allow the reconstruction of a local track segment of the proton trajectory. Each subdetector consists of two coordinate detectors with fibers inclined by $\pm 45^{\circ}$ with respect to the symmetry axis of the $\pm 45^{\circ}$ with respect to the symmetry axis of the plunger vessel. This angle was chosen to avoid a strong bending of the light guide fibers inside the plunger vessel.

Each coordinate detector consists of five fiber layers to ensure good spatial resolution and efficiency. The fibers of 1 mm diameter are positioned in parallel to each other with a pitch of 1.05 mm within each layer. Neighbouring fiber layers are staggered by 0.21 mm to obtain the best spatial resolution.

The size of the fiber detector was chosen to detect most of the scattered protons in one hemisphere of the proton orbit. According to Monte Carlo simulations a detector size

of about $5 \times 5 \text{ cm}^2$ meets this requirement in the vertical stations, while in the horizontal stations detectors of half this size are sufficient. Hence in the vertical stations 48 fibers are combined into one layer while 24 fibers per layer are used in the horizontal stations.

The precision of the fiber positions at the detector end face was measured by a microscope. The typical deviation from the nominal fiber position is $10 \text{ }\mu\text{m}$.

The scintillating fibers are thermally spliced to light guide fibers which transmit the scintillation signals to the PSPMs. The light guides have a length of 50 cm in the vertical stations and 30 cm in the horizontal stations. The light transmission of all spliced connections was measured and only those with a transmission better than 80 % were accepted for the detector production.

To optimize the mechanical stability of the spliced connections the fibers of several producers were tested. The chosen scintillating fibers ³ have an attenuation length of 3.5 m and a trapping efficiency of 4 %. In a test run the light yield of 4.5 photo-electrons per millimeter fiber traversed by a minimum ionizing particle was measured at the end of 2 m light guides [8]. For the detectors in the horizontal stations fibers with double cladding were used. Due to a trapping efficiency of nearly 7 % these fibers have an enhanced light yield.

The light guide fibers are glued into a plastic mask to feed the scintillation signals into the PSPM channels. All fibers of a coordinate detector are combined into the same mask to be read out by one PSPM.

2.3 Position-Sensitive Photo-Multipliers

The position-sensitive photo-multiplier (PSPM) is an efficient device to detect scintillation signals from many fibers simultaneously. Different types of PSPMs are used in the vertical and horizontal stations. For the vertical stations the 64-channel PSPM H4139-20 ⁴ was chosen. This device gave the best results for the readout of the fiber detectors in terms of efficiency and resolution at that time. For the FPS upgrade the 124-channel PSPM MCPM-124 ⁵ was applied in the horizontal stations.

The fundamental difference between the two types of PSPMs is the electron multiplication system. The H4139-20 has a fine-mesh dynode system which gives a gain above 10^6 while the MCPM-124 is equipped with two micro-channel plates which produce a gain typically one order of magnitude less. An important feature of the MCPM-124 is the electro-static focusing and the anti-distortion electrode between the photo-cathode and the first micro-channel plate. Due to the long path of the photo-electrons this device is very sensitive to magnetic fields. A detailed investigation of the micro-channel plate

³POLIFI 02-42-100, Pol.Hi.Tech.,S.P.Turanense Km.44400 - 67061 Carsoli(AQ),Italy.

⁴HAMAMATSU PHOTONICS K.K. Electron Tube Center,314-5 Shimokanzo, 438-0193 Japan.

⁵MELZ, Electrozavodskaja 14, 107061 Moscow, Russia.

PSPM can be found in [9]. The main characteristics of both PSPM types are compiled in table 1.

For the correct recognition of fiber hits the cross talk to neighbouring pixels should be small. The values quoted by the producer range around a few percent. However a large contribution of electronic cross talk can increase the overall cross talk above the level of 10 %.

To read out all 240 fibers of a coordinate detector in the vertical stations by 64 channels of the H4139-20 type implies that 4 fibers have to be coupled to one PSPM pixel. The pixel size of 4 mm diameter is large enough to place 4 fibers of 1 mm diameter without increasing the cross talk. The consequence of this 4-fold fiber multiplexing is a 4-fold ambiguity in the hit recognition. Since the FPS stations aim to measure only one particle track this ambiguity can be resolved by a corresponding segmentation of the trigger planes into four scintillator tiles (section 2.4).

In the horizontal stations all 120 fibers of a coordinate detector can be read out by the 124 channels of the MCPM-124 without multiplexing. The pixel size of $1.5 \times 1.5 \text{ mm}^2$ matches well the fiber diameter of 1 mm. The distortions of the regular anode pixel grid due to the electro-static focusing are compensated by an appropriate design of the fiber mask.

A general principle of the fiber-to-PSPM-pixel mapping is, that neighbouring fibers are not read out by neighbouring PSPM pixels. This scheme reduces the influence of cross talk on the spatial resolution of the detector.

All PSPMs have 2 pixels which are coupled via light guide fibers to light emitting diodes for monitoring and test purposes.

2.4 Trigger Counters

The trigger counters consist of scintillator planes covering the sensitive area of the fiber detectors. Each coordinate detector is equipped with one scintillator plane, placed before or behind the fiber detector. Altogether there are four scintillator planes in each FPS station.

The arrangement of the scintillator planes with respect to the fiber detectors in the vertical stations can be seen in fig.2b. To resolve the spatial ambiguity due to the 4-fold fiber multiplexing the scintillator planes are segmented into four tiles. Each tile covers 12 fibers with a unique fiber-to-PSPM pixel mapping. The trigger tiles are made of 5 mm thick scintillator material BC-408 ⁶. Bundles of 240 light guide fibers of 0.5 mm diameter are used to transmit the light signals to the trigger PMTs. The bundles are glued to the end faces of the scintillator tiles and have a length of 50 cm. Altogether 16 PMTs

⁶BICRON, 12345 Kinsman Road, Newbury, Ohio 44065-9577,USA.

XP1911 ⁷ are used to read out the trigger signals in a vertical station.

In the horizontal stations the scintillator planes are not segmented and only 3 mm thick. Each plane is connected to two bundles of light guide fibers to transmit the scintillation signals to two PMTs R5600 ⁸ - a metal package PMT characterized by compact size and low weight. Since in the horizontal stations the trigger PMTs are placed inside the plunger vessel the light guide bundles have a length of only 15 cm. The main parameters of the trigger PMTs are summarized in table 2.

2.5 Electronics

The main parts of the FPS electronics are given in a block diagram in fig.3. It can be subdivided into three parts:

- the front-end components: preamplifiers and comparators for the signals of the PSPMs and trigger PMTs mounted close to the detectors;
- the conversion, pipelining and trigger electronics located in crates a few meters away from the FPS stations in the HERA tunnel;
- the VME master controller residing outside the HERA tunnel organizing the data read-out and the trigger processing.

In the vertical stations, which are equipped with the H4139-20, one can expect an anode charge of 0.5 pC per fiber hit. A charge sensitive preamplifier with a sensitivity of 1 V/pC is used as the first step in the signal processing chain, followed by a differential driver circuit for common mode rejection. In the horizontal stations the preamplifier sensitivity is enlarged to 30 V/pC due to the lower gain of the MCPM-124. The analog signals of the trigger PMTs are fed into amplifiers to enlarge their amplitudes by a factor of 10 before the digitization.

The first stage of the signal processing is a FADC with 6 bit resolution and 1 V range. It is strobed by the HERA clock and the digitized signals are packed into 8 bit wide pipeline registers. Since HERA has a bunch crossing interval of 96 nsec and the first level trigger decision from the main H1 detector is available only after 2.5 μ sec all data have to be stored in pipelines. The FPS pipeline boards have a length of 32 bunch crossings.

In addition to the FADC readout the signals of the trigger PMTs are fed into comparator boards with a remotely controlled threshold. The output signals are transmitted to the trigger board which compares the hit pattern with trigger conditions consistent with a proton track segment. The logical OR of all conditions comprises the local trigger signal of a FPS station. It is stored together with the hit pattern of all trigger PMTs on

⁷Philips Components, Postbus 90050, 5600 PB Eindhoven, Netherlands.

⁸HAMAMATSU PHOTONICS K.K. Electron Tube Center, 314-5 Shimokanzo, 438-0193 Japan.

the pipeline board.

All local trigger signals are combined to FPS trigger elements for the central H1 trigger processor. To compensate the different distances of the FPS stations to the interaction point programmable delay circuits are used to synchronize the FPS trigger pulses with the HERA clock.

The FPS data are transmitted via a bi-directional fiber optic link to the input FIFO of the VME master controllers. All FPS stations are read out in parallel with a strobe frequency of 5 MHz in a maximum readout time of 52 μsec .

A second fiber optic link is used to transmit the signals from the trigger boards to the VME master controllers outside the HERA tunnel. In the other direction the HERA clock signals and information from the central H1 trigger unit are transmitted to each FPS station.

3 Operation and Data Taking

3.1 Operation of the FPS

The beam profile determines how close the detectors can be moved to the proton beam orbit. It can be calculated from the emittance and the β -function of the proton machine [10]. At the positions of the FPS stations the width and the height of the beam profile are given in table 3. It is a flat ellipse at 90 m and 80.5 m and becomes wider at 64 m.

Assuming a distance of 10 standard deviations of the beam profile plus a safety margin of 2 mm as the closest distance of approach, the detectors in the vertical stations can be moved up to 4 mm to the central proton orbit. In the horizontal stations the distance of closest approach is about 30 mm at 64 m and 20 mm at 80m.

During injection and ramping of the beams all FPS detectors are in their parking positions far from the circulating beam. When stable beam conditions are reached an automatic insert procedure is started. The detectors are moved in steps of 100 μm and the increase of counting rates in the trigger tiles and the beam loss monitors mounted on the beam pipe at 64 m, 83 m and 95 m are observed. For the vertical station at 90 m also the rate of the forward neutron calorimeter [11] located at a distance of 107 m from the interaction point is recorded.

As the detectors are moved towards the proton beam a gradual increase of the rates is observed as long as the plunger vessels remain in the shadow of the HERA machine collimators which cut the tails of the proton beam profile. When the plunger vessel leaves the collimator shadow the rates increase steeply.

The automatic insert procedure evaluates the gradient of the rate increase to stop the movement. If the increase between two consecutive steps exceeds a predefined level the movement is stopped and the detectors have reached their working positions.

The insert procedure starts with the station nearest to the interaction point at 64 m, because particles scattered off the bottom of the plunger vessel affect the rates in the FPS stations further downstream. The whole procedure until all detectors have reached their working positions takes about 20 minutes.

The slow control system records detector parameters in time intervals of seconds and stores them into the database. Some important parameters are the detector positions, the values of the HERA beam position monitors and the trigger rates.

The dose rate in all FPS stations accumulated over one year of HERA operation was measured. At the positions of the fiber detectors the highest rate was 28 krad in the horizontal station at 64 m. The other stations are well protected by the yoke of the BU00 dipole magnet and accumulated doses below 1 krad. The dose rates in all stations are well below the limits of radiation damage of scintillating fibers [12].

An emergency retract system protects the detectors and PSPMs against radiation damage by badly tuned beams or accidental beam loss. When the rate monitors indicate a rate above a critical threshold all detectors are quickly moved to their parking positions.

An important item for the operation of the FPS is the safety of the HERA running. The motor drives of all FPS stations are connected to the H1 emergency power net and in case of a power break all detectors are automatically retracted. In addition, the horizontal stations have a spring loaded sytem to retract the detectors in case of problems. During the detector insert procedure several checks protect the proton beam against accidental detector movement by human intervention or computer failures.

3.2 Data Acquisition Program

The data acquisition (DAQ) has two major tasks: it organizes the data transfer from the front-end electronics to the central H1 event builder and monitors data quality parameters.

When a first level trigger decision stops the filling of the pipeline a controller program starts the readout of the FADC data of a specific set of pipeline stages, which includes all PSPM and trigger PMT signals. The digital trigger data of five consecutive stages are read out including the central pipeline stage containing the FADC data. Due to the long distance to the central H1 detector the signals of a proton traversing the FPS stations reside close to the end of the pipeline.

The master controllers receive the data via a fiber-optical link and perform a pedestal subtraction with zero suppression. Finally, the DAQ program reformats the data for the off-line analysis and sends them to the central event builder.

The size of a typical FPS event is 200 Byte. About 1 % to 2 % of the total H1 data sample contains such an FPS event. The deadtime due to the FPS DAQ is typically 1.2 msec.

The monitor program allows to modify readout parameters as the comparator thresh-

olds of the trigger PMTs, the definition of the trigger conditions, the FADC strobe delays and the zero suppression thresholds of the PSPM amplitudes. In addition it shows control histograms and an online event display.

4 Detector Performance

4.1 Trigger Rate and Efficiency

The trigger rate of the scintillator tiles has contributions from two major sources: the signals from traversing particles, either scattered protons or shower particles from beam-gas or beam-wall interactions, and the background rate due to PMT noise and synchrotron radiation from the electron machine. To reduce the synchrotron background rate all stations are shielded with lead plates.

The majority of the data were recorded with the trigger condition that at least 3 out of 4 trigger planes per station have fired. Moreover, in the vertical stations the combination of scintillator tiles which correspond to a track topology define narrow forward cones. In the horizontal stations the unsegmented scintillator planes are coupled to two PMTs which are used in coincidence to reduce the contribution of PMT noise.

The resulting trigger rates of the vertical FPS stations are between 2 kHz and 4 kHz for typical luminosity conditions with proton and electron currents of 60 mA and 20 mA, respectively. The coincidence rate of the vertical stations varies between 0.5 kHz and 1.5 kHz. In the horizontal stations the trigger rates are significantly higher. This is mostly due to the wide beam profile in the horizontal coordinate (table 3) and the missing shielding of the huge BU00 dipole magnet before the station at 64 m. The typical coincidence rate of the horizontal stations is about 10 kHz.

The four local trigger signals of all FPS stations are combined to 8 FPS trigger elements. They are used in combination with trigger elements from other H1 subdetectors in the central trigger processor. Three physics triggers with the signature of a forward going proton are formed for low multiplicity, photo-production and deep inelastic scattering events.

The efficiency of the trigger tiles is determined from redundant signals which can be attributed to the same forward track. The typical values of the tile efficiency are well above 98 %.

4.2 Hit Identification and Track Reconstruction

The signals of all PSPM channels are classified into hit, noise, or cross talk signals before the track reconstruction.

To reduce the influence of cross talk on the track reconstruction a filter algorithm is applied [13]. Possible cross talk signals in the neighbourhood of channels with large

amplitudes are suppressed, while isolated channels with small amplitudes are kept. A signal above an amplitude threshold of $2 \sigma_i + 1$ FADC counts, where σ_i is the pedestal variation of the i -th PSPM channel, is accepted as a hit if at least one of the two associated trigger tiles has fired.

In the first step of the track reconstruction the fiber hits in a coordinate detector are grouped into clusters compatible with a forward track segment. Hits in at least two layers are requested for each cluster.

As described in section 2.2 each FPS station contains two identical subdetectors separated by 60 mm. Each cluster in the first detector is combined with each cluster in the second detector to obtain a track projection. The slope of these projections is used to select forward going protons. A typical slope distribution with a narrow peak related to forward protons is shown in fig.4a.

Two projections each having at least 5 out of 10 hit layers are combined to a spatial track. A scatter plot of track points in the middle plane between both subdetectors is shown in fig.4b. Only very few fake tracks due to misidentified track projections or ambiguous combinations in multi-track events can be seen outside the sensitive detector area.

All spatial tracks inside the sensitive detector area are used to form global tracks for each pair of vertical and horizontal FPS stations. Before this step the track points have to be corrected for the detector positions. The large distance between two FPS stations allows to measure the slopes of global tracks with an accuracy of a few μrad .

For a minimum multiplicity of 5 fiber hits the probability to find a local track projection is 86 %. This results in a reconstruction efficiency of about 50 % for protons passing both vertical stations. In the horizontal stations this efficiency is smaller due to the lower layer efficiency (section 4.3).

4.3 Fiber Detector Efficiency and Resolution

The performance of the fiber detectors is described by the layer efficiency, which is defined as the probability that a fiber layer indicates a hit if it is traversed by a charged particle. The layer efficiency depends on the light yield, the attenuation of the scintillating and light guide fibers, and losses in the readout chain and the hit finding algorithm. Another source of inefficiency is the dead material between neighbouring fibers. Assuming an effective fiber core diameter of 900 μm the geometrical layer efficiency is 86 % for a fiber pitch of 1050 μm .

The hit multiplicity of reconstructed tracks is used to evaluate the layer efficiencies. For a typical run range the layer efficiencies of all FPS stations are shown in fig.5. In the vertical stations the values vary between 50 % and 80 % with an average around 65 %. In the horizontal stations the layer efficiencies are slightly lower. They range from 30 %

to 70 % with an average around 50 %. The lower values in the horizontal stations can be explained by the lower quantum efficiency and gain of the MCPM-124, as given in table 1. In all FPS stations a degradation of the layer-efficiencies between 5 % and 10 % per year was observed. Possible reasons are the aging of PSPMs and fiber detectors, intensified by the synchrotron radiation and beam induced background during injection and beam steering in the HERA tunnel. To maintain the quality of the FPS stations fiber detectors with too low layer-efficiency and PSPMs with a gain degradation were exchanged during the accelerator shut-down periods.

The spatial resolution of the fiber detectors is determined by the overlap region of hit fibers in subsequent layers. Due to the 210 μm staggering of fibers in neighbouring layers a theoretical resolution of 60 μm can be obtained if all fibers are 100 % efficient. In practice this resolution is deteriorated by inefficient fibers, noise hits and the dead material between the fibers.

For a horizontal station the measured spatial resolution as a function of the hit multiplicity is shown in fig.6. The average value of the resolution is 150 μm , in good agreement with results from prototype measurements at the DESY electron test beam [8]. Due to the different combinations of overlapping fibers a particular hit multiplicity results in overlap regions of different sizes. This effect propagates into the variance of the resolution which starts for all multiplicities around 100 μm and ranges up to 300 μm for the lowest multiplicities.

The spatial detector resolution has to be compared with the uncertainty of the proton trajectory due to vertex smearing and beam divergence at the interaction point. Depending on the proton energy these sources give an additional uncertainty between 50 μm and 150 μm at the positions of the FPS stations. The Coulomb scattering of a proton passing a FPS station results in an uncertainty of similar size in the stations further downstream. Due to these inevitable contributions, the total resolution cannot be significantly improved by a better spatial resolution of the fiber detectors.

4.4 Energy and Angle Reconstruction

The energy reconstruction is based on the knowledge of the optics of the proton beam line [10]. Since only dipoles and quadrupoles are placed between the interaction point and the FPS stations the deflections in the horizontal and vertical projections are decoupled. This allows the energy of the scattered proton to be reconstructed independently in both projections.

The coordinate system in the following description is defined by a horizontal X -axis, a vertical Y -axis and a Z -axis pointing in beam direction. The intercept X and slope X' of global tracks in the horizontal projection are related to the energy E and the scattering angle Θ_x of the proton at the interaction point by two linear equations:

$$X = a_x(E) + b_x(E) \cdot \Theta_x \quad (1)$$

$$X' = c_x(E) + d_x(E) \cdot \Theta_x \quad (2)$$

A corresponding set of equations holds for the vertical projection. The transfer functions $a_x(E)$, $b_x(E)$, $c_x(E)$ and $d_x(E)$ are determined from Monte Carlo simulations of forward protons at the reference positions $Z = 85$ m and $Z = 72$ m for the vertical and horizontal stations respectively.

While the reconstruction in the horizontal projection has a unique solution for energy and angle, the vertical projection has two solutions in most cases. In the vertical stations a large fraction of these double solutions has unphysically large scattering angles and can thus be rejected. For the remaining tracks the solution with the energy closer to the energy found in the horizontal projection is accepted. The final proton energy is the weighted average of the energies from both projections.

The energy spectrum of scattered protons measured with the vertical FPS stations during 1996 data taking with 820 GeV proton beam energy is shown in fig.7a. It begins around 500 GeV and drops sharply above 750 GeV. The upper edge of the energy spectrum reflects the fact that in both vertical station the closest distance of approach to the circulating proton beam is about 4 mm.

The errors of the reconstructed energies are shown in fig.7b. The mean error is 6 GeV at 700 GeV proton energy and decreases to 2 GeV for protons at 500 GeV.

To evaluate the absolute energy scale error, the FPS measurements were compared with predictions of the proton energy from the central H1 detector. Events with a high photon virtuality, where the hadronic final state is well contained in the central detector, were used for this purpose. Based on a sample of 17 events we estimate an energy scale error of 10 GeV [14].

The reconstructed spectra of the polar angles Θ_x and Θ_y of scattered protons are shown in fig.7c,d. The acceptance in the vertical stations is limited to values $|\Theta_{x,y}| < 0.4$ mrad corresponding to transverse momenta $p_T < 300$ MeV/c. The mean error of the Θ_x measurement is 5 μ rad independent from the proton energy, while the mean error of Θ_y increases from 5 μ rad at 500 GeV up to 100 μ rad at 700 GeV.

4.5 Calibration of the Detector Positions

The transfer functions in (1) and (2) are calculated with respect to the nominal beam orbit. Since the actual beam orbit varies for different proton fills, a fill-dependent calibration of the detector positions is necessary before the track parameters can be used for the energy reconstruction. This calibration is based on the comparison of global tracks with a Monte Carlo sample using the nominal beam optics.

Fig.8a shows the scatter plot of intercepts X and slopes X' of global tracks in the horizontal projection at the reference position $Z = 85$ m before the calibration. Superimposed are the lines of constant energy and scattering angles assuming the nominal interaction point and beam optics. Certain combinations of X and X' are forbidden, but this region is partly occupied by uncalibrated tracks. This discrepancy is based on the difference between nominal and actual beam orbit and can be improved by additional offsets for slopes and intercepts of global tracks - the calibration constants ΔX and $\Delta X'$. They are determined in a maximum likelihood fit minimizing the number of tracks in the forbidden region. Fig.8b shows the scatter plot after the calibration with much less tracks in the forbidden region.

In the vertical projection the same scheme is applied. Due to the shape of the scatter plot a unique solution of the calibration constants ΔY and $\Delta Y'$ can only be found if the energy measurement in the horizontal projection is used as an additional constraint.

In the horizontal FPS stations the calibration can be done in a similar way. In addition, the diffractive photo-production of ρ -mesons [15], where the final state is completely measured in the central detector and the FPS, offers an independent method to check the energy scale.

5 Summary and Outlook

For the H1 experiment at the HERA collider a spectrometer was built to measure forward protons with energies greater than 500 GeV in the angular range below 1 mrad with respect to the proton beam direction. Such protons escape the central detector through the beam pipe and can be detected at a large distance from the interaction point where their positions deviate a few millimeters from the circulating proton beam.

The FPS consists of two vertical stations at 81 m and 90 m which approach the beam from above and two horizontal stations at 64 m and 80 m which approach the beam from the outer side of the HERA ring.

The main components of the FPS are fiber detectors located in Roman Pots, which can be moved close to the proton orbit. The detectors consist of 5 staggered layers of scintillating fibers of 1 mm diameter. The scintillating fibers are spliced to light guide fibers which transmit the signals to position-sensitive photo-multipliers. For triggering each FPS station is equipped with four planes of scintillator tiles.

The fiber detectors in the vertical FPS stations have a spatial resolution of $150 \mu\text{m}$ and a typical layer-efficiency of 65 %. This allows the proton trajectory to be reconstructed through both stations for about 50 % of the triggered events. In the horizontal FPS stations the spatial resolution is as good as in the vertical stations, but the layer-efficiency is slightly less, typically 50 %.

The local track elements are combined into global tracks for the pairs of vertical and

horizontal FPS stations. The parameters of these global tracks are used to evaluate the energy and scattering angle of the proton at the interaction point. The deflection of scattered protons in the horizontal and vertical projection is decoupled and the energy can be measured twice. For 820 GeV proton beam energy the vertical stations measure scattered protons in the energy range between 500 GeV and 750 GeV. The corresponding error varies between 2 GeV and 6 GeV for the lowest and highest energies respectively, with an additional energy scale error of 10 GeV.

The kinematic range of the horizontal FPS stations is complementary to that of the vertical stations. The horizontal stations give access to the diffractive region with $x_{\mathbb{P}} < 0.1$, where $x_{\mathbb{P}} = 1 - E'/E_p$ is the fractional energy of the exchange. This is illustrated in fig.9.

Until 1999 an integrated luminosity of about 15 pb^{-1} was collected with the vertical stations and 5 pb^{-1} with the horizontal FPS stations. First physics results for the structure function with a leading proton have been published from the 1995 data with the vertical stations [16]. The semi-inclusive structure function $F_2^{LP(3)}$ with leading protons in the kinematic range $580 \text{ GeV} < E' < 740 \text{ GeV}$ and $p_T < 200 \text{ MeV}$ was measured [17]. In another analysis the photo-production cross section with leading protons and two jets was evaluated and compared to theoretical predictions [18].

Acknowledgement

The technical help provided by the workshops of the DESY laboratories at Hamburg and Zeuthen is gratefully acknowledged. In particular we thank the technicians H.J.Seidel and P.Pohl. The continuous assistance of the HERA machine, survey and vacuum groups is essential for the successful operation of the Roman Pot devices. We thank D.P.Johnson (Brussels), B.Stella (Rome) and J.Zsembery (Saclay) for their help in the early phase of this project. This project was supported by the INTAS-93-43 grant.

References

- [1] H1 Collaboration, I.Abt et al., Nucl.Instr.and Meth.A386 (1997) 310, ibid.348.
- [2] H1 Collaboration, T.Ahmed et al., Phys.Lett.B348 (1995) 681;
H1 Collaboration, S.Aid et al., Nucl.Phys.B463 (1996) 3;
H1 Collaboration, S.Aid et al., Nucl.Phys.B468 (1996) 3;
H1 Collaboration, S.Aid et al., Nucl.Phys.B472 (1996)3, ibid.32.
- [3] T.Regge, Nuovo Cimento 14 (1959) 951;
G.Chew and S.Frautschi, Phys.Rev.Lett.7 (1961) 394;
A.Kaidalov, Phys.Rep.50 (1979) 157;
K.Goulianos, Phys.Rep.101 (1983) 169;
A.Donnachie and P.Landshoff, Phys.Lett.B296 (1992) 227.
- [4] G.Alberi and G.Goggi, Phys.Rep.74 (1981) 1;
G.Chew, S.Frautschi and S.Mandelstam, Phys.Rev.126 (1962) 1202;
A.W.Thomas and C.Boros, ADP-98-79/T346,hep-ph/9812264v2, 1999.
- [5] G.Ingelmann and P.Schlein, Phys.Lett.B152 (1985) 256;
A.Donnachie and P.Landshoff, Nucl.Phys.B303 (1988) 634.
- [6] ZEUS Collaboration, M.Derrick et al., Phys.Lett.B356 (1995) 129;
H1 Collaboration, C.Adloff et al., Z.Phys.C76 (1997) 613;
H1 Collaboration, "Measurement of the diffractive structure function F_2^{D3} at low and high Q^2 at HERA", contr. paper to the 29th Int.Conf.on High Energy Physics ICHEP'98, Vancouver, Canada, 1998.
- [7] U.Amaldi et al., Phys.Lett.43B (1973) 231;
R.Battiston et al., Nucl.Instr.and Meth.A238 (1985) 35;
A.Brandt et al., Nucl.Instr.and Meth.A327 (1993) 412;
F.Abe et al., Phys.Rev.D50 (1994) 5518;
ZEUS Collaboration, J.Breitweg et al., Eur.Phys.J.C2 (1998) 246.
- [8] J.Bähr et al., DESY preprint 92-176, 1992;
J.Bähr et al., DESY preprint 93-200,93-201, 1993;
J.Bähr et al., Nucl.Instr.and Meth.A330 (1993) 103;
J.Bähr et al., Nucl.Instr.and Meth.A371 (1996) 380.
- [9] J.Bähr et al., DESY-Zeuthen preprint 95-01, 1995.
- [10] D.C.Carey, "The Optics of Charged Particle Beams", Harwood Academic Publishers, New York, 1987;
K.G.Steffen, "High-Energy Beam Optics", Interscience Monographs and Texts in

Physics and Astronomy, Vol.17, John Wiley and Sons, New York, 1995;
 K.Wille, "Physik der Teilchenbeschleuniger und Synchrotronstrahlungsquellen", Teubner, Stuttgart, 1992;
 J.Roßbach and P.Schmüser, "Basic course on accelerator optics", DESY preprint M-93-02, 1993.

[11] M.Beck et al., Nucl.Instr.and Meth.A381 (1996) 330;

T.Nunnemann, Thesis MPIH-V7-1999, University of Heidelberg, 1998.

[12] C.Zorn, Nucl.Phys.B32 (1993) 377;

J.Bähr et al., DESY preprint 99-079, 1999, physics/9907019.

[13] The filter algorithm corrects the measured amplitudes S_i by subtracting the weighted amplitudes of the direct and diagonal neighbours according to:

$$\hat{S}_i = 1.025 \left(S_i - 0.15 \sum_{dir.} S_j - 0.10 \sum_{diag.} S_j \right)$$

[14] H1 Collaboration, "The Forward Proton Spectrometer of H1", contr.paper pa17-025 to the 28th Int.Conf. on High Energy Physics ICHEP'96, Warsaw, Poland, 1997.

[15] H1 Collaboration, C.Adloff et al., Z.Phys.C75 (1997) 607;

H1 Collaboration, C.Adloff et al., DESY 99-010, 1999, hep-ex/9902019, subm.to Eur.Phys.J.C.

[16] H1 Collaboration, C.Adloff et al., Eur.Phys.J.C6 (1999) 587.

[17] B.List, Thesis, University of Hamburg, 1996.

[18] C.Witteck, Thesis, University of Hamburg, 1997.

Table 1: Typical parameters of the position-sensitive photo-multipliers H4139-20 and MCPM-124 used in the vertical and horizontal FPS stations, respectively.

Characteristics	H4139-20	MCPM-124
photo-cathode material	bi-alkaline	multi-alkaline
window	glass	fiber optic
size	$40 \times 40 \text{ mm}^2$	25 mm diam.
quantum efficiency at 400 nm	typ. 20 %	typ. 15 %
dynode structure	proximity mesh	micro-channel plates
stages	16	2
anode pixels	8 x 8	10 x 10 + 4 x 6
pixel pitch	5.08 mm	2.2 mm
pixel size	4 mm diam.	$1.5 \times 1.5 \text{ mm}^2$
max.voltage	2.7 kV	2.9 kV
gain	10^6 at 2.5 kV	3×10^5 at 2.8 kV
pulse time	2.7 nsec rise	2.5 nsec total
uniformity	1 : 3	1 : 3
average cross talk	1 %	1 - 2 %

Table 2: Typical parameters of the trigger photo-multipliers XP1911 and R5600 used in the vertical and horizontal FPS stations, respectively.

Characteristics	XP1911	R5600
photo-cathode material	bi-alkaline	bi-alkaline
window	glass	glass
size	15 mm diam.	8 mm diam.
quantum efficiency at 400 nm	20 %	20 %
dynode structure	linear focused	metal channel
stages	10	8
max.voltage	1.9 kV	1.0 kV
gain	10^6 at 1.2 kV	10^6 at 0.8 kV
pulse time	2.3 nsec rise	0.65 nsec rise

Table 3 : The horizontal and vertical profile of the 820 GeV proton beam at the interaction point and at the positions of the FPS stations in terms of standard deviations σ_x and σ_y of a Gaussian parametrization. For the emittance the value 17π mm · mrad was assumed.

z / m	σ_x /mm	σ_y /mm
0	0.17	0.05
64	2.49	0.82
80.5	1.86	0.25
90	1.38	0.22

Figure Captions

- Fig.1** A schematic view of forward beam line a) in the horizontal b) in the vertical projection indicating the 10σ beam envelope, the main magnets and the FPS stations at 64 m, 80 m, 81 m and 90 m.
- Fig.2** A horizontal FPS station a) with fiber detectors in parking position and a vertical FPS station b) showing the fiber detector end faces and the scintillator planes of the trigger counters.
- Fig.3** The electronic scheme : the PSPM and trigger PMT signals are transmitted via optical links to the VME master controllers - in the other direction control signals (HERA clock, pipeline enable , fast clear) are sent to the FPS stations.
- Fig.4** The local tracks in a horizontal FPS station: a) a slope spectrum with the peak signal of forward proton tracks, b) spatial track points with the shape of the detector area.
- Fig.5** The layer efficiencies of the fiber detectors a,b) in the vertical stations during 1996 data taking and c,d) in the horizontal stations during 1998 running.
- Fig.6** The spatial resolution of the fiber detectors in the horizontal stations in dependence on the multiplicity of fiber hits. The bars describe the variance according to the different sizes of the fiber overlap regions for combinations with the same hit multiplicity.
- Fig.7** The energy and angular spectra measured with the vertical FPS stations in 1996 a) the energy E obtained from the measurements in both projections, b) the error ΔE in dependence on the energy E , and the polar angles c) Θ_x , and d) Θ_y .
- Fig.8** The scatter plots of intercepts X and slopes dX/dZ of global tracks in the vertical stations a) before and b) after the calibration of the detector positions. The full lines correspond constant energies from 420 GeV to 820 GeV, the dashed lines are for constant angles from -0.7 mrad to $+0.7$ mrad.
- Fig.9** The geometrical acceptance in dependence on the fractional momentum $x_{\mathbb{P}}$ of the exchange for protons passing a) the vertical and b) the horizontal FPS stations.

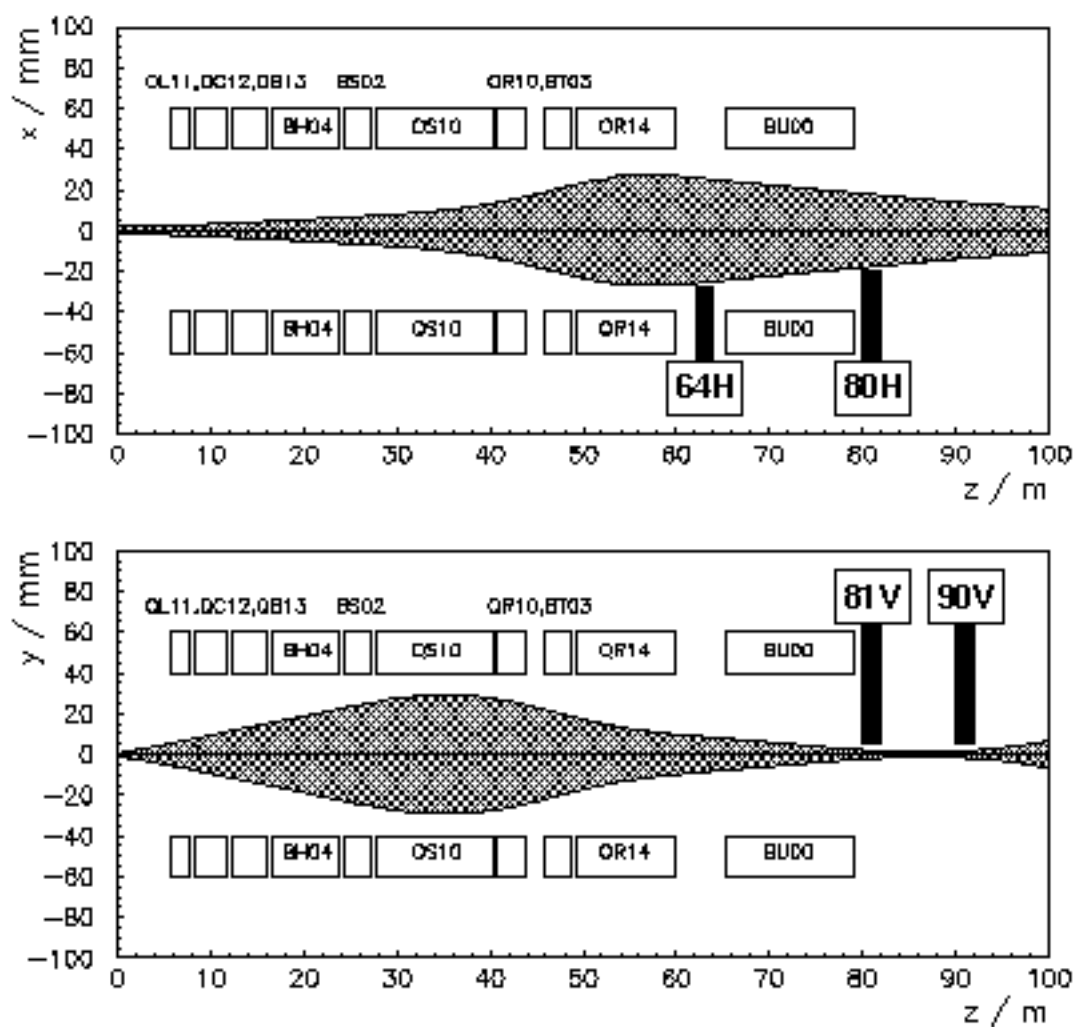


Fig. 1

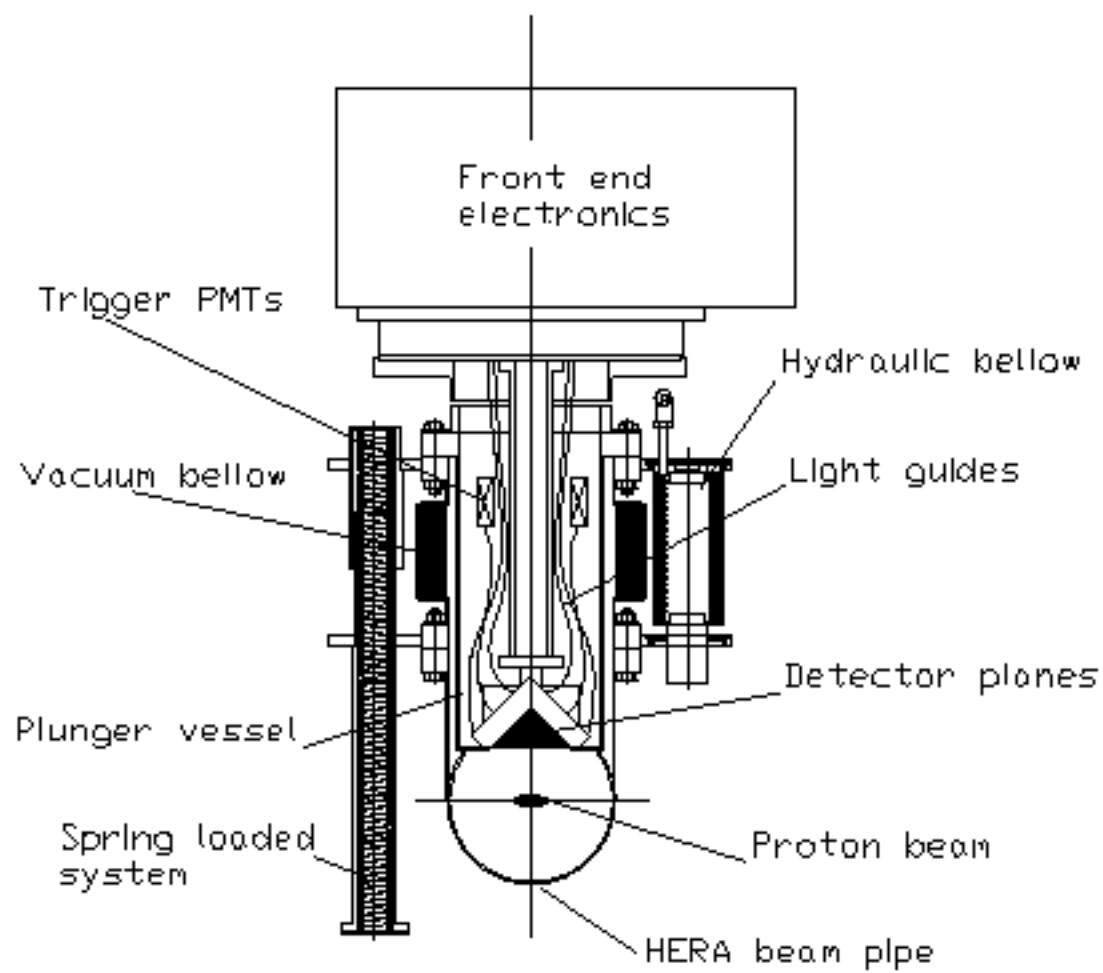


Fig. 2a

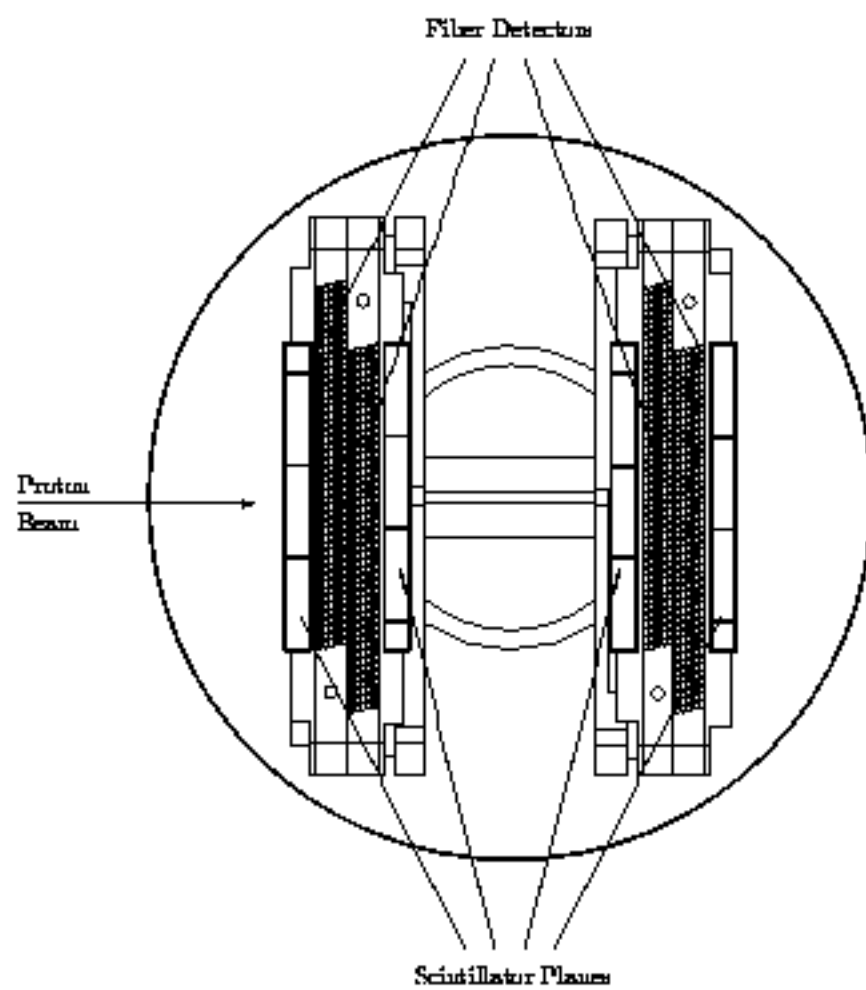


Fig. 2b

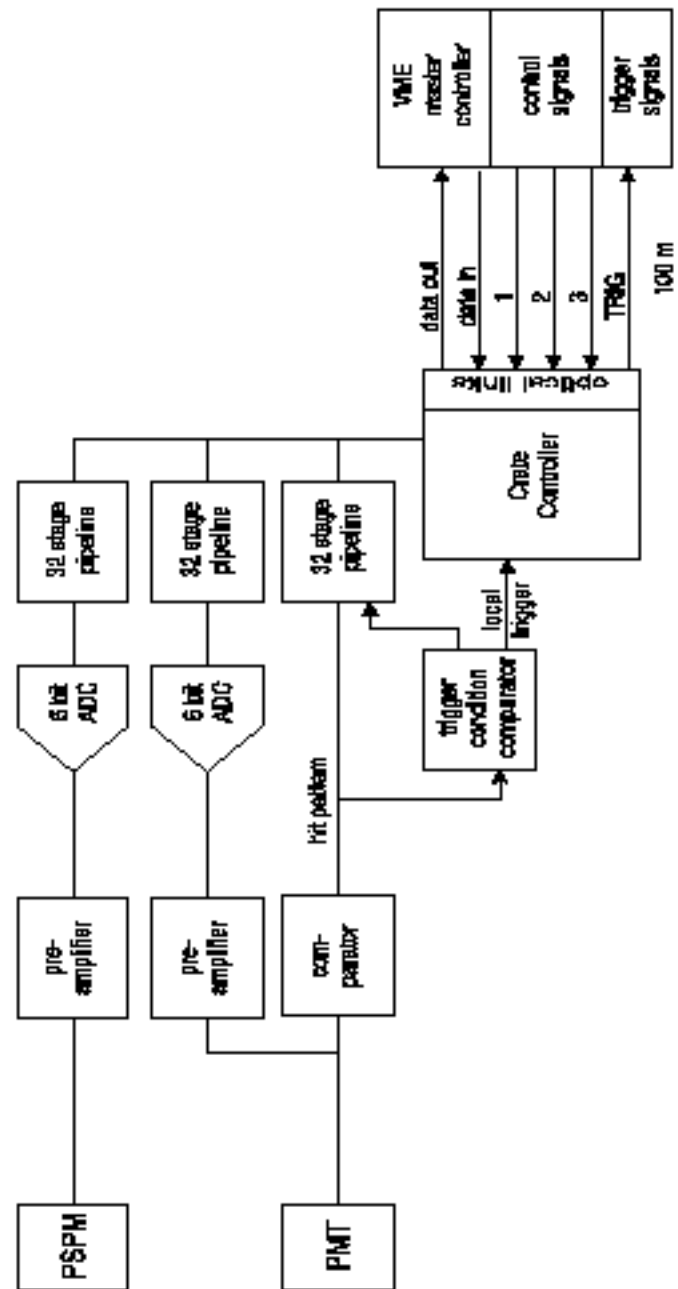


Fig. 3

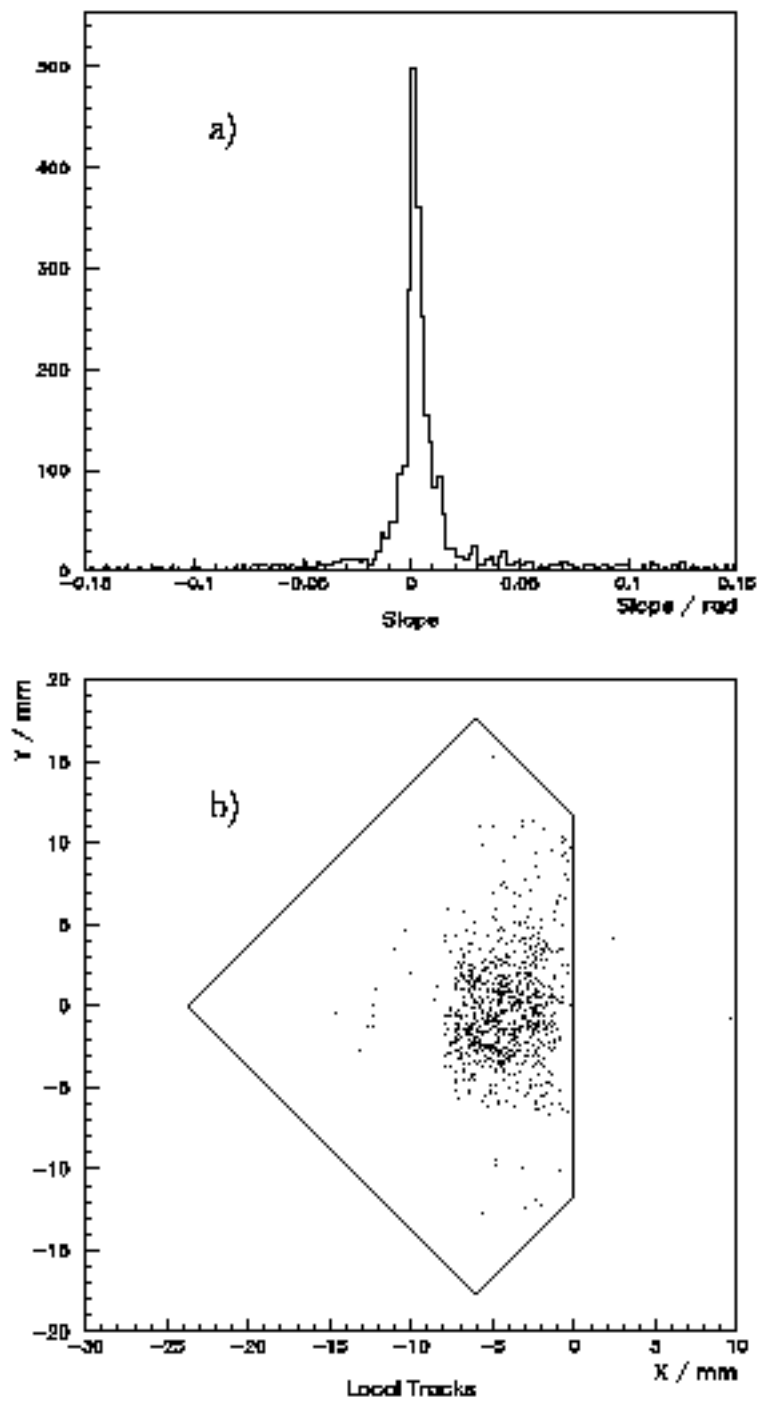


Fig. 4

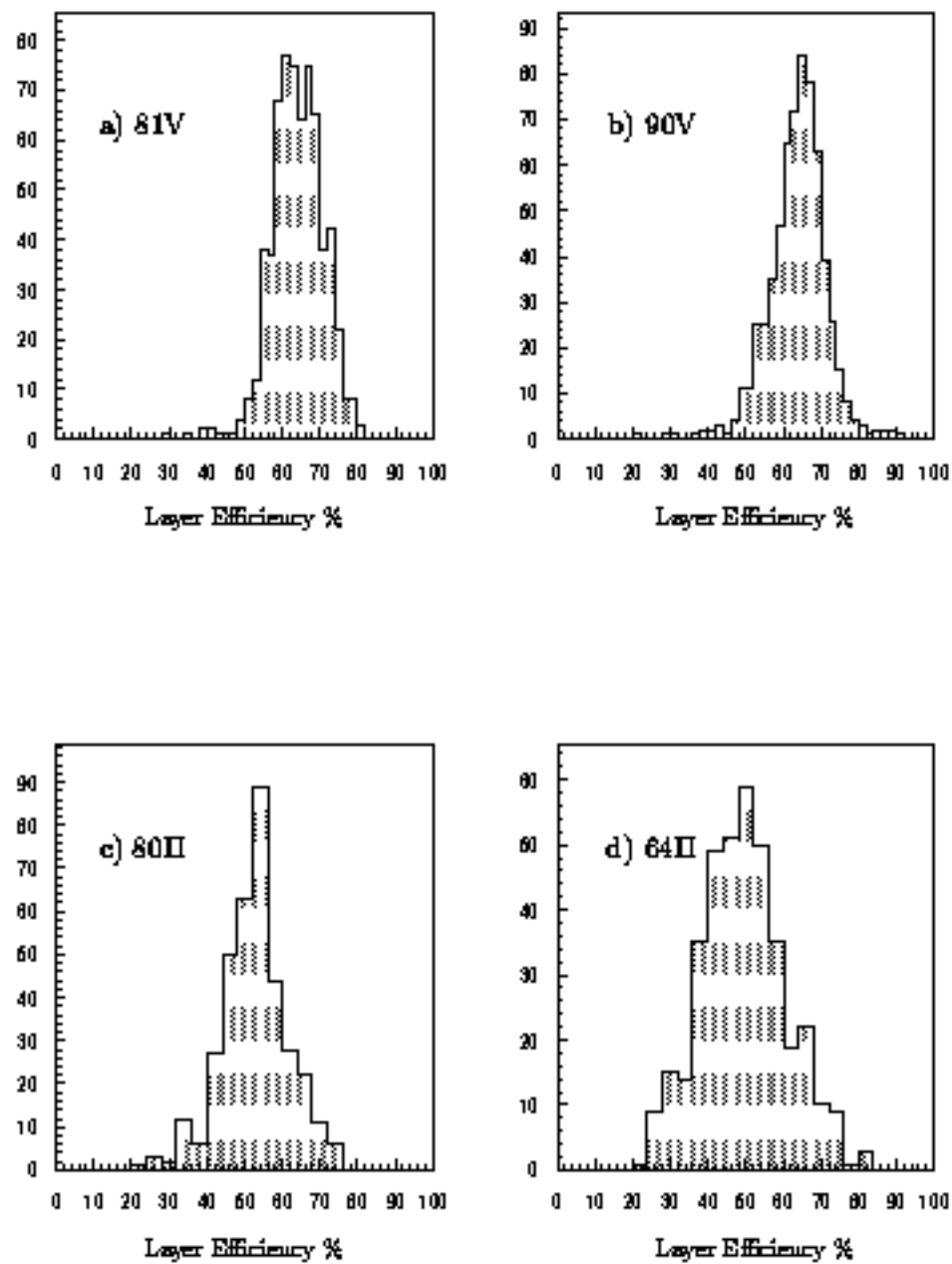


Fig. 5

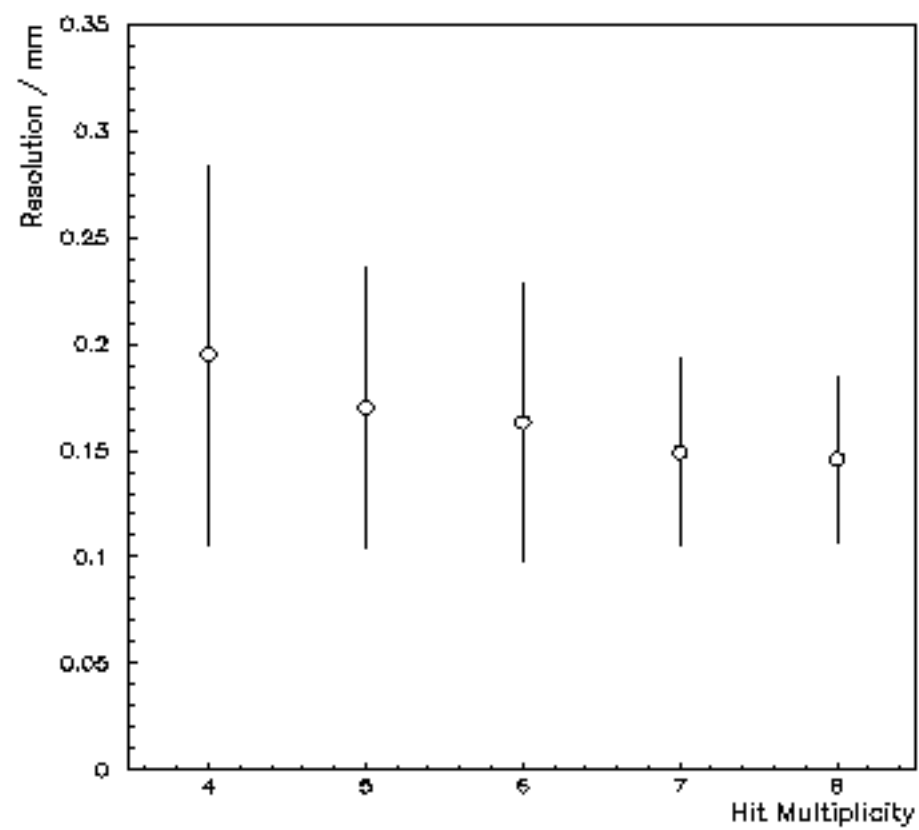


Fig. 6

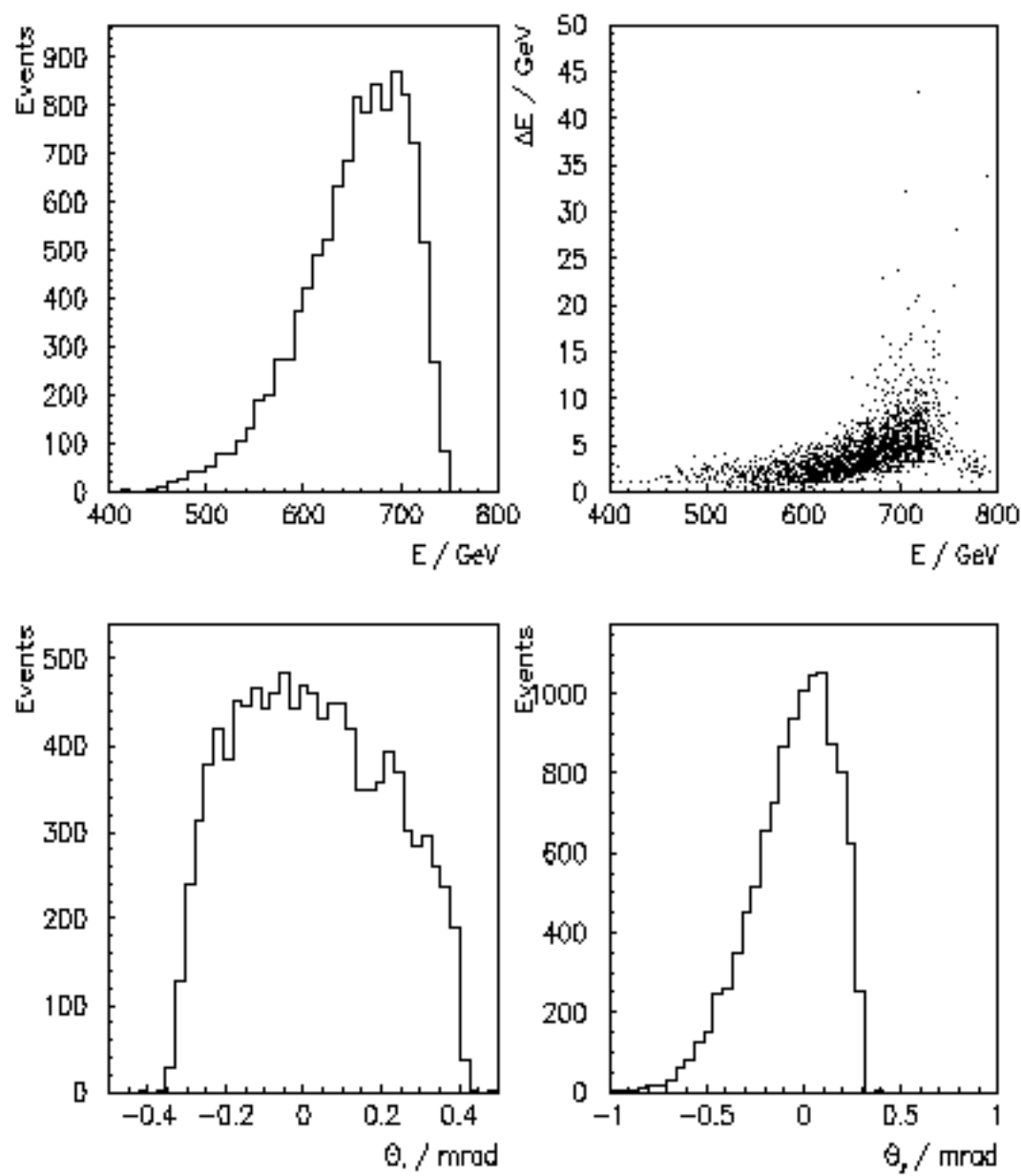


Fig.7

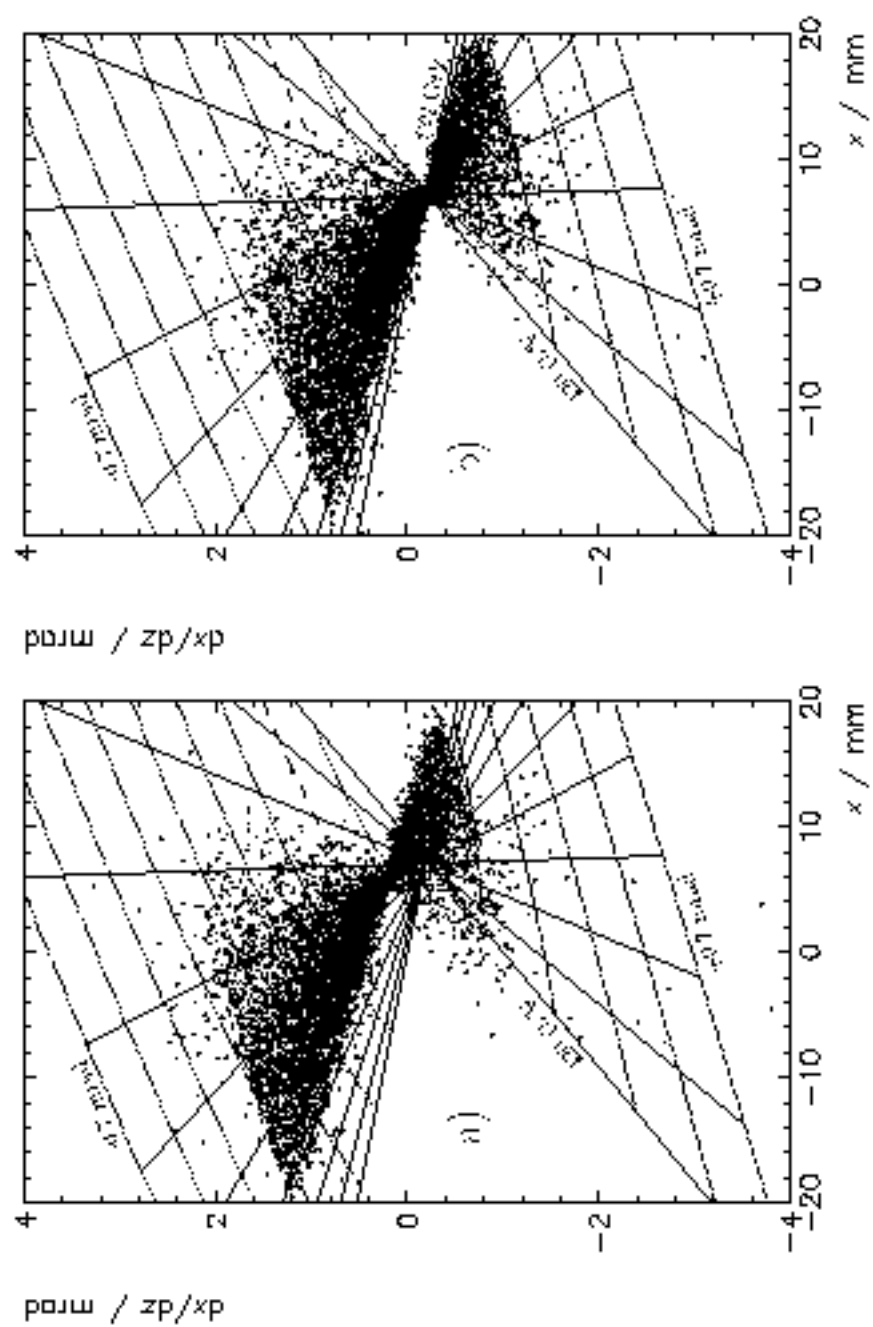


Fig.8

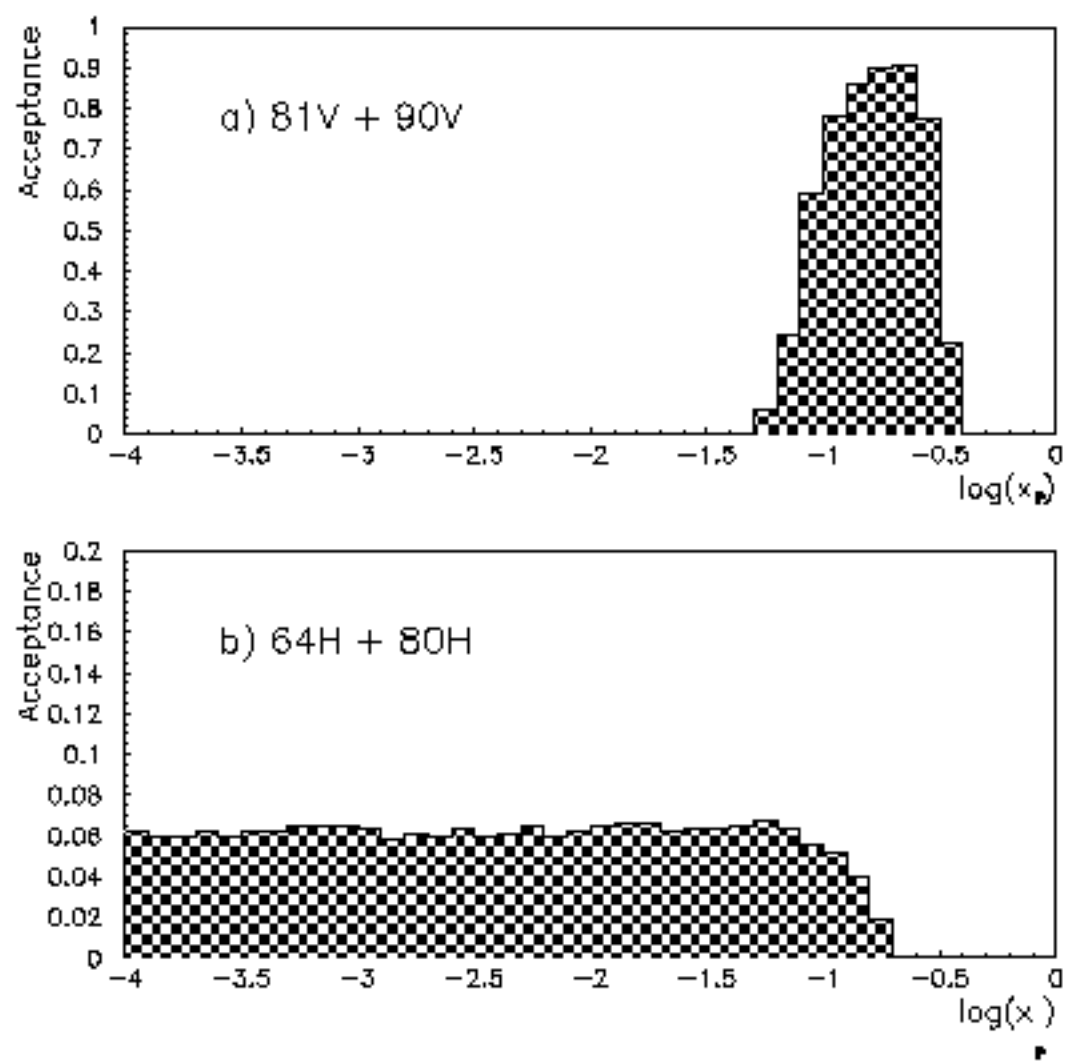


Fig.9